# Tailoring Diesel Bioblendstock from Integrated Catalytic Upgrading of Carboxylic Acids: A "Fuel Property First" Approach

| | |
|---|---|
| Journal: | *Green Chemistry* |
| Manuscript ID | GC-ART-05-2019-001820.R1 |
| Article Type: | Paper |
| Date Submitted by the Author: | 11-Aug-2019 |
| Complete List of Authors: | Huo, Xiangchen; National Renewable Energy Laboratory, ; Colorado School of Mines, Civil and Environmental Engineering<br>Huq, Nabila; National Renewable Energy Laboratory<br>Stunkel, Jim; National Renewable Energy Laboratory<br>Cleveland, Nicholas; National Renewable Energy Laboratory, National Bioenergy Center<br>starace, Anne; National Renewable Energy Laboratory,<br>Settle, Amy; National Renewable Energy Laboratory, National Bioenergy Center<br>York, Allyson; National Renewable Energy Laboratory; Colorado School of Mines, Department of Chemistry<br>Nelson, Robert; National Renewable Energy Lab, National Bioenergy Center<br>Brandner, David; National Renewable Energy Laboratory,, National Bioenergy Center<br>Fouts, Lisa; National Renewable Energy Laboratory,<br>St. John, Peter; National Renewable Energy Laboratory, Biosciences Center<br>Christensen, Earl; National Renewable Energy Laboratory, Center for Transportation Technologies and Systems<br>Luecke, Jon; National Renewable Energy Laboratory<br>Mack, J. Hunter; Univ Massachusetts<br>McEnally, Charles; Yale University, Chemical and Environmental Engineering<br>Cherry, Patrick; Yale University, New Haven, USA, chemical engineering<br>Pfefferle, Lisa; Yale University,<br>Strathmann, Timothy; Colorado School of Mines, Civil and Environmental Engineering<br>Salvachua, Davinia; National Renewable Energy Laboratory, National Bioenergy Center<br>Kim, Seonah; National Renewable Energy Laboratory, National Advanced Biofuels Consortium; National Renewable Energy Laboratory, National Bioenergy Center<br>McCormick, Robert; National Renewable Energy Laboratory,<br>Beckham, Gregg; National Renewable Energy Laboratory, National Bioenergy Center<br>Vardon, Derek; National Renewable Energy Laboratory, National Bioenergy Center |

SCHOLARONE™
Manuscripts

# Tailoring Diesel Bioblendstock from Integrated Catalytic Upgrading of Carboxylic Acids: A "Fuel Property First" Approach

Xiangchen Huo[a,b], Nabila A. Huq[a], Jim Stunkel[a], Nicholas S. Cleveland[a], Anne K. Starace[a], Amy E. Settle[a,b], Allyson M. York[a,b], Robert S. Nelson[a], David G. Brandner[a], Lisa Fouts[a], Peter C. St. John[a], Earl D. Christensen[a], Jon Luecke[a], J. Hunter Mack[c], Charles S. McEnally[d], Patrick A. Cherry[d], Lisa D. Pfefferle[d], Timothy J. Strathmann[b], Davinia Salvachúa[a], Seonah Kim[a], Robert L. McCormick[a], Gregg T. Beckham[a], Derek R. Vardon[a]*

[a]National Renewable Energy Laboratory, 15013 Denver West Parkway, Golden, CO, United States
[b]Colorado School of Mines, 1500 Illinois St., Golden, CO, United States
[c]University of Massachusetts Lowell, 220 Pawtucket St., Lowell, MA, United States
[d]Yale University, 9 Hillhouse Avenue, New Haven, CT, United States
*Derek.Vardon@nrel.gov

## Abstract

Lignocellulosic biomass offers the potential to produce renewable fuels at a scale commensurate with petroleum consumption. Hybrid approaches that combine biological and chemocatalytic processes have garnered increasing attention due to their flexibility for feedstock utilization and diversity of potential products. Of note, lignocellulosic sugars can be converted biologically to short-chain carboxylic acids, while subsequent chemocatalytic upgrading can elongate the carbon backbone and remove oxygen from the structure to produce drop-in hydrocarbon fuels. However, hybrid conversion processes are typically not designed with the fuel properties in mind *a priori*. In this work, we apply a "fuel property first" design approach to produce a tailored hydrocarbon bioblendstock with lower intrinsic sooting and drop-in diesel fuel potential. Initially, model predictions for six fuel properties critical to diesel applications (physicochemical requirements, energy content, safety considerations, autoignition ability, and sooting tendency) were used to screen an array of hydrocarbons accessible from upgrading individual and mixed $C_2/C_4$ acids. This screening step allowed for down-selection to a non-cyclic branched $C_{14}$ hydrocarbon (5-ethyl-4-propylnonane) that can be synthesized from butyric acid through sequential catalytic reactions of acid ketonization, ketone condensation, and hydrodeoxygenation. Following evaluation of each conversion step with model compounds, butyric acid was then converted through an integrated catalytic process scheme to achieve >80% overall carbon yield to a hydrocarbon mixture product containing >60% of the target $C_{14}$ hydrocarbon. The potential of this conversion strategy to produce a hydrocarbon diesel bioblendstock from lignocellulosic biomass was then demonstrated using corn stover-derived butyric acid produced from *Clostridium butyricum* fermentation. Experimental fuel property testing of the purified $C_{14}$ blendstock validated the majority of the fuel property model predictions, including <50% of the intrinsic sooting tendency when compared to conventional diesel. Meanwhile, the crude conversion product met fuel property target metrics, validating conversion process development. When the $C_{14}$ bioblendstock was blended into a petroleum diesel at 20 vol.%, the blend maintained low cloud point, high energy density, and cetane number. Notably, the blend reduced sooting tendency by more than 10%, highlighting the potential of the tailored bioblendstock to reduce particulate emissions.

## Introduction

Biofuels have the potential to offset environmental impacts of the transportation sector, which accounts for 55% of oil consumption and 23% of energy-related $CO_2$ emissions globally.[1, 2] Passenger vehicles rank number one in consumption of oil, closely followed by road freight vehicles. Due to technology advances such as electrification, oil demand for passenger vehicles has begun to plateau, but the demand of oil (primarily diesel) for road freight vehicles is projected to continue rising over the next few decades.[3] Therefore, identifying routes to sustainable diesel fuel production is particularly important to both meeting future demand and curbing climate change. Lignocellulosic biomass is a relatively low-cost feedstock that allows renewable fuels to be produced at a meaningful scale.[4] A wide array of molecules can be accessed from lignocellulosic biomass through diverse conversion pathways (e.g., biochemical, thermochemical, hybrid),[5-7] creating ample opportunities to produce biofuels. A rational fuel design approach can have a major impact on enhancing the value proposition of biofuels.

Computational tools have seen growing application in multiple product development fields to reduce time, manpower, and cost.[8-10] For example, computer-aided molecular design leverages quantitative structure–property relationships (QSPRs) and numerical optimization algorithms to search for optimal molecular structures across massive design space that includes completely novel structures.[11] In the context of biofuel development, computational screening of potential fuel molecules can greatly facilitate experimental study by enabling fuel candidate down-selection to identify the most promising synthesis targets.[12, 13] This process is enabled by fuel property predictive models, which provide estimates of fuel characteristics relevant to its handling and application, such as physical and chemical properties (e.g., density, boiling point, and C/H/O composition). Models specifically related to fuel performance have received increasing attention and can provide valuable information for designing performance-advantaged fuel molecules. Examples include octane number (ON) and cetane number (CN), which describe fuel antiknock quality and autoignition ability, respectively.[14] In addition, with the growing concern of soot emissions on climate change and negative impacts to human health,[15, 16] new tools are emerging for the design of clean burning fuels. Yield sooting index (YSI) is one such computational and experimental tool that was shown to correlate with traditional smoke point measurement.[17, 18] Experimentally, YSI has the benefit of minimal sample requirement (~100 uL) which allows for rapid screening, predictive model development,[19, 20] and reduced barriers when studying novel molecules. As such, significant potential remains for applying YSI to advance the design of clean-burning biofuels.

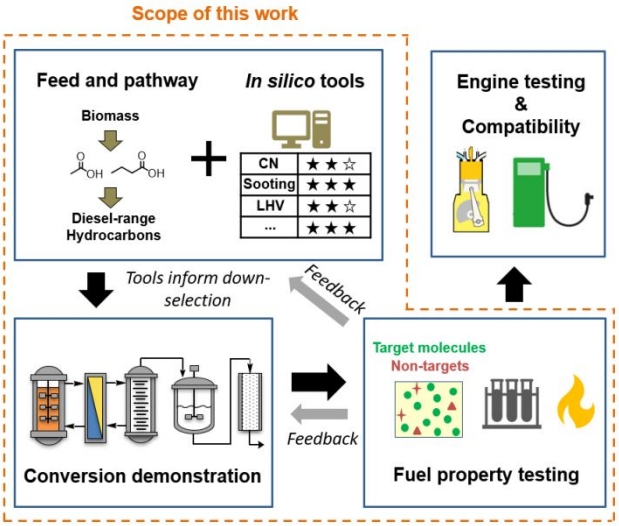


**Scheme 1.** "Fuel property first" design approach to leverage fuel property predictive models for the design of performance-advantaged diesel bioblendstock.

Hybrid conversion processes integrating biochemical and chemocatalytic processes provide multiple routes to access promising fuel molecules from biomass. Of note, short-chain carboxylic acids have received growing interest as platform molecules. They can be produced in high yield from the low-cost anaerobic fermentation of lignocellulosic sugars and waste streams.[21-26] Meanwhile, carboxylic acid group functionality allows for diverse chemocatalytic chemistries to extend the carbon chain length and reduce oxygen content, resulting in fuel-range molecules. For example, recent efforts have identified catalysts and reaction parameters for converting carboxylic acids to ketones, alcohols, and hydrocarbons of higher carbon number and diverse connectivity (e.g., linear, branched, cyclic, unsaturated/aromatic) through a combination of C-C coupling, dehydration, and hydrogenation chemistries.[27-31] However, the viability of the conversion products as fuel was evaluated to a much less extent, potentially due to limited product quantity from conversion studies. Particularly, the sooting behavior of these biofuels was unaddressed. Efficient evaluation of these fuel candidates can be facilitated by computational tools, which remain underutilized.

To address these gaps, we demonstrate a "fuel property first" design approach to guide the development of high-quality, low-sooting diesel bioblendstocks from short-chain carboxylic acids (**Scheme 1**). This approach utilizes *a priori* computational screening of long-chain hydrocarbon molecules accessible from the catalytic upgrading of acetic and butyric acid. The hydrocarbon functionality was targeted to take advantage of its compatibility with existing fuel infrastructure that would allow it to be deployed in the near term as a drop-in blendstock.[32, 33] Prediction and evaluation of critical fuel properties, including the sooting tendency metric YSI, informed target molecule down-selection for further conversion pathway development. Catalytic conversion efforts evaluated both single-step conversion and an integrated catalytic process scheme using model carboxylic acids, with the integrated scheme further demonstrated using carboxylic acids derived from the anaerobic fermentation of corn stover hydrolysate. The produced hydrocarbon diesel blendstocks were experimentally verified to display fuel properties in line with model predictions and shown to readily reduce the sooting tendency when blended into commercial diesel. Results from this work provide justification for future process scale-up and engine performance evaluation. Broadly, the "fuel property first" approach can be applied to other feedstocks, conversion

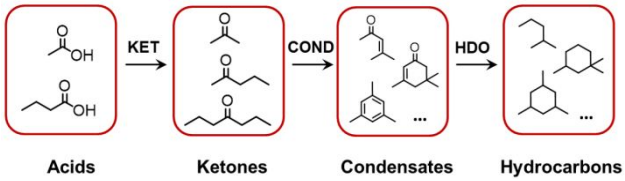


**Scheme 2** Upgrading scheme for converting $C_2/C_4$ carboxylic acids to hydrocarbon molecules via ketonization (KET), condensation (COND), and hydrodeoxygenation (HDO).

chemistries, and fuel applications to accelerate the development and adoption of renewable, clean burning bioblendstocks.

# Results

## *Fuel Property Prediction*

### *Mapping Hydrocarbons Derived from $C_2/C_4$ Acids*

Fermentation-derived acetic acid and butyric acid were selected for combinatorial screening since they can be anaerobically produced from mixed lignocellulosic sugars in high yields.[22, 34] Hydrocarbons with potential to be generated from upgrading individual and mixed $C_2/C_4$ carboxylic acids were then mapped using a multi-step catalytic conversion route consisting of ketonization, condensation, and hydrodeoxygenation (HDO) (**Scheme 2**). Ketonization reacts two carboxylic acids to extend their carbon chain-length by forming a ketone with the release of $CO_2$ and $H_2O$.[35, 36] Self-ketonization of acetic acid and butyric acid generates acetone and 4-heptanone, respectively, while cross-ketonization between these two acids generates 2-pentanone. The ketone carbon backbone can be further elongated by condensation reactions that form non-cyclic branched dimers and cyclic trimers, while fully retaining all carbon and releasing oxygen in the form of water.[37] Lastly, HDO converts condensation products to hydrocarbons, with dimers resulting in non-cyclic branched hydrocarbons and trimers resulting in cyclic hydrocarbons.[27, 30, 37] Overall, the reaction mapping process resulted in 30 hydrocarbons spanning from $C_6$ to $C_{21}$ (**Table S1**). While most of these hydrocarbons displayed carbon numbers within the range of diesel fuel ($C_{10}$ to $C_{25}$),[38] their fuel properties were evaluated computationally to determine their dependence on molecular structure.

Fuel properties of the hydrocarbons were estimated using predictive models and compared against target metrics to identify desirable molecules and structures. These properties concern multiple aspects of fuel deployment, including physicochemical requirements, energy content, safety considerations, and emission potential. Starting with low-temperature handling ability, a fuel with an adequate regional and seasonal applicability requires a low melting point (or low cloud point for mixtures). A maximum value of 0°C was used for initial screening.[39] Using predictive models based on group contribution and correlation,[40, 41] the non-cyclic branched hydrocarbons were all anticipated to exhibit low melting points (<-30°C) suitable for cold environments, while cyclic hydrocarbons of $C_{15}$ or larger risk failing to meet the requirement. Similarly, efficient fuel utilization must also satisfy a boiling point requirement, because non-volatile compounds resist evaporation/burning and remain in-cylinder, causing long-term operation issues. This fuel criterion was defined to be <338°C, consistent with the maximum allowable T90 specified for petroleum diesel by ASTM D975.[42] Except for $C_{21}$ molecules, group contribution methods[40, 41, 43] predicted that all of the hydrocarbons evaluated herein meet this requirement. Meanwhile, low boiling point compounds cause safety concerns because they may form a flammable fuel-air mixture above the liquid. To ensure the safe handling and storage of a fuel, a minimum flash point of 52°C is specified for general purpose diesel by ASTM D975 and employed as a screening criterion in current study.[42] Molecules of $C_{11}$ and above in both non-cyclic branched and cyclic hydrocarbon groups were predicted to meet this requirement using correlations built from fuel and hydrocarbon databases,[44, 45]. Generally, a positive trend with carbon number was observed for these three fuel properties (**Figure S1a-c**), as expected for paraffinic hydrocarbons.[46-48]

Energy density, which is essential to fuel economy, was quantified by the lower heating value (LHV) of each compound. This is a measure of the heat released by combusting a quantity of fuel, minus the heat of vaporization of the combustion-generated water. LHV varies between 32-44 MJ $kg^{-1}$ for petroleum diesel, and a value of 40 MJ $kg^{-1}$ was selected as the minimum requirement to ensure a competitive energy density. Utilizing models correlating heats of combustion with elemental analysis,[49-51] all mapped hydrocarbon molecule predictions fell well above the LHV requirement and were nearly uniform (**Figure S1d**) due to similarities in elemental composition (e.g., 84-86 wt.% carbon).

The autoignition and sooting behavior of the hydrocarbons were informed by predicting CN and YSI using machine learning methods.[19, 52, 53] For CN, a higher value indicates faster autoignition, which in turn can improve heat release rates and engine cold-start capabilities. The minimum requirement of 40, in line with ASTM D975 requirements, was selected to ensure adequate fuel reactivity,[42] although CN requirements can vary depending on the region (e.g., a minimum CN of 51 required by DIN EN 590 in Europe[54]). Nine non-cyclic branched hydrocarbon molecules and two cyclic hydrocarbon molecules were predicted to meet the minimum requirement of 40 (**Table S1**). Previous studies have shown that CN increases with the secondary C-H:primary C-H ratio due to a lower-energy alkylperoxy radical isomerization pathway enabled by secondary C-H bonds.[55-57] However, the absence of a strong correlation in this study (**Figure S1e**) suggested significant influence from tertiary C-H and/or quaternary carbon as well.[58]

In contrast to autoignition ability, soot emission from diesel combustion currently does not have a known verified predictive fuel property metric. Diesel combustion is largely mixing-controlled, and soot formation is likely to depend on intrinsic sooting tendency, ignition delay, and physical properties relative to spray penetration and breakup. For this initial screening, YSI was chosen to assess the sooting potential of fuel candidates, with the higher value denoting stronger chemical sooting tendency.[19] Predicted YSI of the mapped hydrocarbons was shown to generally increase with carbon number in **Figure S1f**. YSI normalized by carbon number characterizes the average contribution of each carbon atom in the molecule to soot formation and was roughly constant for each category of hydrocarbons (see last column of **Table S1**). For the non-cyclic branched hydrocarbons, normalized YSI values varied between

5.9–6.8 and were lower than those of the cyclic hydrocarbons (7.3–9.0). The stronger sooting tendency of the cyclic structure agrees with experimental observations in the literature,[59] as small cyclic hydrocarbons tend to have lower energy barrier pathways towards forming resonantly-stabilized soot precursors.[60]

***Down-selection of Targets for Diesel Blendstock***

Based on these predicted fuel properties, a subset of $C_{12}$–$C_{14}$ molecules was identified to contain promising diesel candidates, including four non-cyclic branched hydrocarbon molecules and one cyclic hydrocarbon molecule (**Table 1**). These molecules are accessed from either single $C_4$ acid or mixed $C_2/C_4$ acids. With butyric acid, the $C_{14}$ hydrocarbon in **Table 1** can be synthesized from self-condensation of 4-heptanone that is generated from butyric acid ketonization. When mixed $C_2/C_4$ acids are used, acetone and 2-pentanone are formed in addition to 4-heptanone, which provides a pathway to all five of the down-selected molecule candidates. However, the presence of acetone and 2-pentanone negatively impacts the ability to selectively produce the target hydrocarbon molecules due to their facile condensation into cyclic trimers that react to form cyclic hydrocarbons after HDO.[27, 30, 37] As noted, the resulting cyclic hydrocarbons display less desirable diesel fuel properties, such as low CN and high YSI. Therefore, we chose to focus on the conversion pathway that starts solely with butyric acid targeting the non-cyclic branched $C_{14}$ hydrocarbon, 5-ethyl-4-propylnonane, shown in the first entry of **Table 1**. Previous studies have shown proof-of-concept for the individual catalytic conversion steps comprising this pathway.[30, 37] As such, this work looked to evaluate the integrated catalytic conversion scheme and validate diesel blendstock properties for both the target $C_{14}$ hydrocarbon and crude conversion product.

## *Catalytic Upgrading of Butyric Acid*

***Single Step Conversion of Model Compounds***

Initially, each catalytic conversion step in the butyric acid upgrading scheme was evaluated individually for conversion efficiency and carbon yield with the aim of moving towards process relevant conditions. The ketonization reaction was first performed using commercial butyric acid (≥99% purity, Sigma Aldrich) in a continuous flow reactor to remove the corrosive acid functional group and increase the $C_4$ carbon chain length to $C_7$, producing $CO_2$ and water in the process. The reactor was packed with a commercial $ZrO_2$ catalyst, which is an amphoteric redox metal oxide known to provide high activity and selectivity for this chemistry.[61] The catalyst displayed a surface area of 65 $m^2$ $g^{-1}$ and total acidity of 163 μmol $g^{-1}$ (**Table S2**). At 435°C and a weight hourly space velocity (WHSV) of 3.8 $h^{-1}$, butyric acid was completely converted for over 11 hours of time-on-stream with an overall mass recovery >92% (**Figure 1**). The gas phase product was primarily $CO_2$, and the condensable liquid product was biphasic due to the low water solubility of 4-heptanone (approx. 3 g $L^{-1}$ at room temperature). The purity (refers to mass purity in this study) of 4-heptanone in the organic liquid phase was 90%. Although the non-target products were not fully identified, work was conducted to determine the impact of these compounds on the integrated catalytic upgrading steps and final fuel properties, as discussed below.

**Table 1** Model predictions of melting point, boiling point, flash point, lower heating value (LHV), cetane number (CN), and yield sooting index (YSI, normalized to carbon number in parentheses) for down-selected hydrocarbon molecules. Average values reported when multiple predictions are available. Full list of molecule candidates and model predictions provided in **Table S1**.

| Hydrocarbons | C No. | Melting point (°C) | Boiling point (°C) | Flash point (°C) | LHV (MJ/kg) | CN | YSI |
|---|---|---|---|---|---|---|---|
| Screening criteria | None | <0 | <338 | >52 | >40 | >40 | None |
| 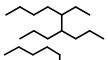 | 14 | -38 | 241 | 82 | 45 | 48 | 91 (6.5) |
| 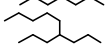 | 12 | -48 | 204 | 62 | 45 | 45 | 71 (5.9) |
| | 12 | -61 | 199 | 61 | 45 | 44 | 75 (6.2) |
| 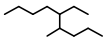 | 12 | -61 | 199 | 61 | 45 | 43 | 75 (6.2) |
| | 13 | -24 | 231 | 84 | 45 | 44 | 99 (7.6) |

Aldol-type condensation was then performed on the 4-heptanone product stream to further elongate the carbon chain to $C_{14}$ and reduce the oxygen content. While significant work has been performed to date with terminal ketones,[27, 62, 63] condensation of internal ketones, such as 4-heptanone, is far less studied. Recently, $Nb_2O_5$ was identified as a highly selective catalyst (>80% carbon selectivity) to the dimer (mixture of positional and stereoisomers) for 4-heptanone condensation, but the chemistry has only been demonstrated for single-pass batch reactions with 8 wt.% of 4-heptanone in toluene.[16, 21] When considering process design impacts, the relatively low ketone loading will require large equipment and high energy consumption for solvent separation. Therefore, we evaluated conversion efficiency at elevated ketone loadings with catalyst regeneration and recycle (**Figure 2**).

4-Heptanone condensation was performed in a bench-scale batch reactor. A commercial $Nb_2O_5$ catalyst acquired from CBMM was calcined at 350°C prior to use, resulting in a surface area of 137 $m^2$ $g^{-1}$ and total acidity of 255 μmol $g^{-1}$ (**Table S2**). Initial experiments were performed using commercial 4-heptanone (98% purity, Sigma Aldrich) with a

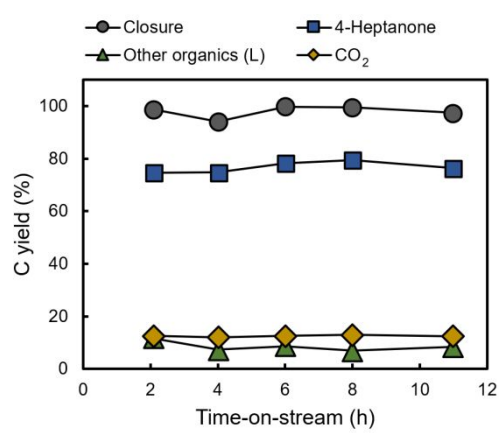


**Figure 1** On-stream performance and product distribution for commercial butyric acid (neat) ketonization over $ZrO_2$. Ketonization conditions: catalyst loading 3 g, Ar flow 100 sccm at 1 atm, bed temperature 435°C, WHSV 3.8 $h^{-1}$ based on butyric mass flow rate.

ketone loading of 20 wt.% in toluene, ketone-to-catalyst mass ratio of 4:1, reaction temperature of 180°C, and an initial atmospheric pressure He headspace. Under these conditions, conversion progressed rapidly in the first 3 h to 27% and then gradually to 58% after 24 h (**Figure S2a**). At 24 h, selectivity to the desired dimer was 81%, similar to previous studies.[16, 21] Identification and quantification of dimer was based on GC-FID/MS (**Figure S3** and **S4**). The turnover number was well above unity, confirming that the reaction is catalytic (**Figure S2b**). The overall mass recovery was >98% with neglible mass loss to the gas phase, and the carbon mass recovery was >96%. The reactivity of 4-heptanone is significantly lower compared to that of the terminal ketone, as demonstrated for example by conversion of 2-heptanone reaching 90% in the first 3 h under similar conditions (data not shown). The lower reactivity is likely due to steric hinderance, making internal ketones inherently more difficult to process.

To assess catalyst recyclability, spent $Nb_2O_5$ was washed with solvent, dried, and tested under the same reaction conditions as the fresh catalyst. Continuous decline in activity was observed in subsequent reuses (**Figure S2c**), likely due to incomplete removal of adsorbed species. A carbon content of 2.3 wt.% was measured for spent $Nb_2O_5$ after 24 h reaction, suggesting fouling as a mode of deactivation. Calcination of the spent catalyst in air at 350°C for 12 h was then employed to regenerate the catalyst. Over four cycles of reuse, a 15% decrease in dimer carbon yield was observed (**Figure 2**). Surface area and total acidity of the regenerated catalysts showed insignificant change compared to those of the fresh catalyst, while small quantities of carbon residue were measured on the regenerated catalysts (**Table S3**). These observations suggest that the most active sites are vulnerable to deactivation and like not fully regenerated under mild conditions. Although carbon residue can be removed at higher calcination temperatures, further evaluation of catalyst activity will be needed as increasing temperature can lead to loss of water content and phase transition, accompanied by reduced surface area and acidity for this catalyst.[64]

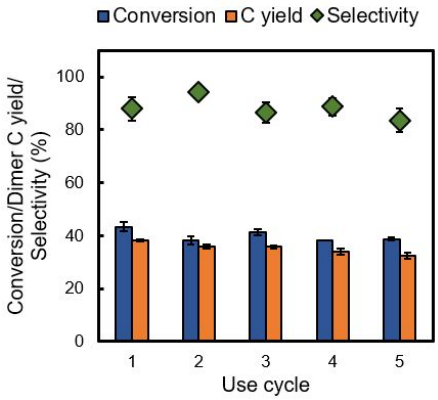


**Figure 2** $Nb_2O_5$ reuse for 4-heptanone condensation in a batch reactor with oxidative regeneration between cycles. Condensation conditions: 15 g feed comprised of 20 wt.% 4-heptanone in toluene, 0.75 g catalyst, initial He headspace at atmospheric pressure, 180°C, 10 h, stirring 800 rpm. Regeneration conditions: furnace temperature 350°C, static air, 12 h.

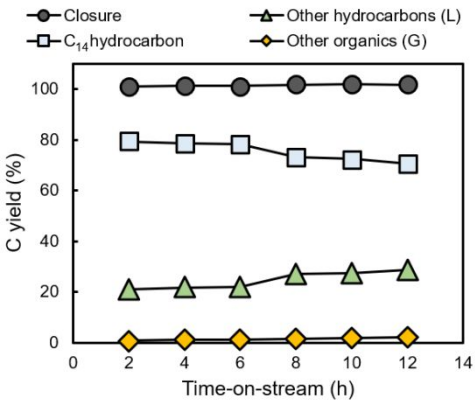


**Figure 3** On-stream performance and product distribution for condensation dimer (neat) HDO over 3 wt.% $Pt/Al_2O_3$. HDO conditions: catalyst loading 1 g, $H_2$ flow 165 sccm at 500 psi, bed temperature 334°C, WHSV 4.4 $h^{-1}$ based on dimer mass flow rate. The dimer HDO feed (81% dimer purity) was generated from commercial 4-heptanone condensation following distillation to remove solvent and recover product.

Additional reaction conditions were then evaluated to further reduce solvent use and improve single-pass conversion by increasing the ketone loading (20 wt.% to 100 wt.%), catalyst loading (catalyst-to-ketone mass ratio from 1:20 to 1:5), and operating temperature (180°C to 220°C). When the ketone loading increased from 20 wt.% to 100 wt.% (i.e., neat solvent-free) for a given catalyst loading, 10 h conversion decreased (**Figure S5a**), while the turnover number was nearly constant (**Figures S5b**), indicating a high coverage of surface intermediates at these ketone loadings.[65] Increasing the catalyst loading under neat conditions increased dimer concentration in the liquid product (**Figure S5c**) but also enhanced carbon loss to catalyst surface. For example, 0.04 g carbon was measured for the spent catalyst at a catalyst-to-ketone mass ratio of 1:20, and this value increased more than three-fold to 0.13 g when the mass ratio increased to 1:5. With respect to operating temperature, raising the temperature from 180°C to 220°C at 20 wt.% ketone loading increased conversion by 30% after 10 hours of reaction but reduced dimer selectivity by 20% (**Figure S6a**). Estimating the activation energy from Arrhenius plots was hindered (**Figure S6b**), with one possible reason being accelerated carbon laydown at higher temperature. Although beyond the scope of this study, high temperature processing of neat internal ketones requires further analysis to evaluate the tradeoff between increased conversion at the expense of selectivity and final fuel properties.

The final HDO step was then examined to convert the purified dimer into the target $C_{14}$ hydrocarbon. The dimer feed was derived from commercial 4-heptanone and prepared by removing the reaction solvent and unreacted ketone through distillation, resulting in a mixture of 81% dimer and 19% non-target compounds. The latter may include higher boiling point trimer and larger oligomers that we were unable to identify by GC (**Figure S7**). HDO was performed in a packed bed flow reactor using a 3.3 wt.% $Pt/Al_2O_3$ catalyst due to its metal-acid bifunctionality.[66, 67] The catalyst displayed a surface area of 198 $m^2\ g^{-1}$, metal dispersion of 9.4%, and total acidity of 329 µmol $g^{-1}$, with the latter dominated by Lewis acidity (**Table S2**). At 334°C and a WHSV of 4.4 $h^{-1}$, the dimer was completely converted with >97% overall mass recovery and >90% selectivity to a $C_{14}$ hydrocarbon based on incoming dimer purity (**Figure 3**). Deoxygenation of the feed was also complete, resulting in a biphasic product comprising an organic phase (85 wt.% C and 15 wt.% H) and an aqueous phase. The $C_{14}$ hydrocarbon was confirmed to exhibit the target structure by a combination of high-resolution mass spectrometry (**Figure S8**) and nuclear magnetic resonance spectroscopy (**Figure S9**). A 10% decrease in $C_{14}$ hydrocarbon carbon yield was observed over 12 hours of time-on-stream due to an increasing degree of isomerization and cracking of the $C_{14}$ hydrocarbon. The spent $Pt/Al_2O_3$ catalyst contained 5.5 wt.% carbon, relatively small (<0.2%) compared with the total carbon mass processed. Regeneration by calcination completely restored the catalyst physicochemical properties (**Table S4**), indicating catalyst fouling as the likely cause for the decrease in $C_{14}$ hydrocarbon carbon yield. Additional test of the catalyst at partial conversion conditions is needed to evaluate deactivation kinetics. Future work is also required to understand the impact of deactivation on reaction network and consequent change of product distribution.

***Integrated Conversion of Model and Bio-butyric Acid***

Although the individual catalytic conversion steps above were demonstrated to have relatively high selectivity (>80%) towards target products, the formation of non-target compounds poses additional challenges when using a fuel design approach based on evaluation of individual compounds. To this end, butyric acid was upgraded through the integrated catalytic conversion scheme shown in **Scheme 3**. Starting with a model butyric acid feed, the ketonization resulted in complete butyric acid conversion with 13% carbon converted to $CO_2$ and 78% carbon converted to 4-heptanone (**Figure 4**). While the formation of $CO_2$ was stoichiometric and consistent with complete acid conversion, carbon yield to 4-heptanone was 88% of the theoretical carbon yield. The remaining 9% of the carbon was retained in non-target byproducts primarily in the same phase as 4-heptanone. The organic phase of the liquid product was then decanted for separation from water. Note that carryover of water to the next conversion step may not affect process efficiency as the $Nb_2O_5$ catalyst used for ketone condensation is water tolerant.[30, 68]

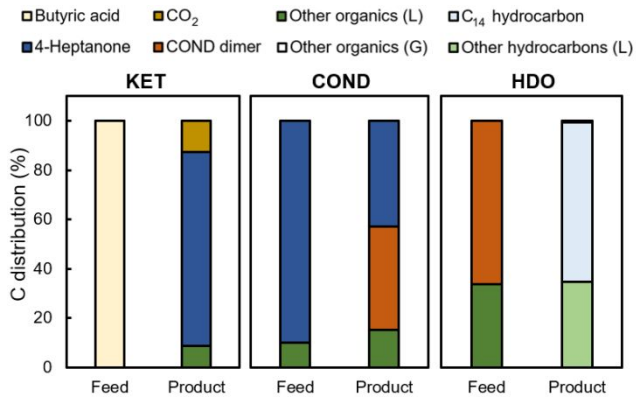


**Figure 4** Carbon distribution for each conversion step when integrating ketonization, condensation, and HDO to upgrade commercial butyric acid. Experimental conditions identical with **Figure 1**, **Figure S2a** (24 h reaction), and **Figure 3,** with the exception that HDO time-on-stream was 2 h due to limited sample.

The ketonization organic phase was then mixed with toluene at 20 wt.% for the condensation reaction under the conditions shown in **Figure S2a**. After 24 h, conversion of 4-heptanone reached 55% with an 82% selectivity to the dimer, nearly identical to the results obtained with commercial 4-heptanone (58% conversion and 81% selectivity). Due to byproduct formation during condensation, the fraction of carbon in the non-target compounds increased from 10% to 15% after the reaction (**Figure 4**). The reaction product was distilled to separate the dimer and heavier byproducts from solvent and unreacted ketone. Three fractions were obtained from distillation (**Figure S10a**), where solvent and unreacted ketone were primarily recovered in fractions 1 and 2. Condensation performed on the recycled solvent and ketone over two cycles exhibited comparable 4-heptanone conversion

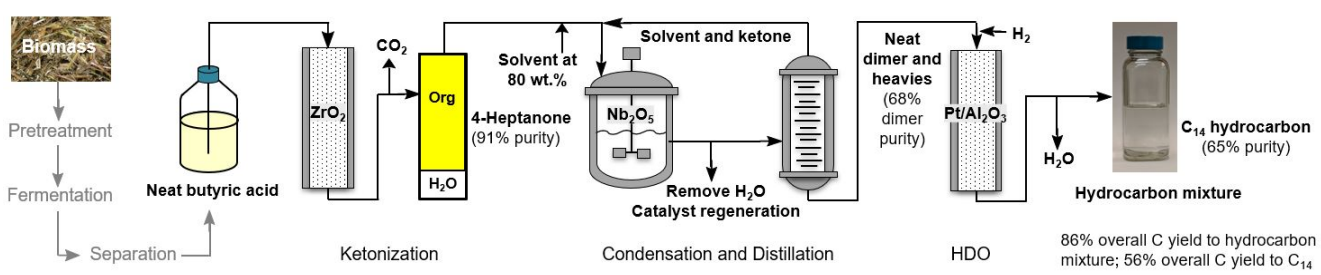


**Scheme 3** Integrated process scheme for upgrading butyric acid to hydrocarbon diesel blendstock. The overall carbon yield calculation for the hydrocarbon mixture product following HDO and the target $C_{14}$ hydrocarbon assumed ideal separation and mass recovery, with continuous recycle of unreacted 4-heptanone following condensation (see **Figure S10** for ketone recycling). See **Table 2** for target reactants conversion and target products carbon yield for each reaction step. Purity of conversion intermediates (4-heptanone and dimer) and target $C_{14}$ hydrocarbon refers to mass purity.

**Table 2** Conversion of target reactants (i.e., butyric acid, 4-heptanone, condensation dimer) for the reaction steps of KET, COND, and HDO, respectively, with associated carbon yields to target products when upgrading commercial and biologically-derived butyric acid.

| Conversion step | Bio-acid | | Commercial acid | |
|---|---|---|---|---|
| | Conversion | C yield | Conversion | C yield |
| KET[a] | 100% | 76% | 100% | 77% |
| COND[b] | 54% | 42% | 55% | 45% |
| HDO[c] | 100% | 88% | 100% | 97% |

[a]KET reaction conditions identical to **Figure 1** for commercial acid. Shorter time-on-stream (1.8 h) used for bio-butyric due to limited sample.
[b]COND reaction conditions identical to the 24-h reaction in **Figure S2a** for single-pass 4-heptanone conversion.
[c]HDO reaction conditions identical to **Figure 3** with C yield reported at 2 h of time-on-stream for commercial feed; bio-feed prepared by diluting the dimer distillation fraction in cyclohexane at 20 wt.% due to limited sample quantity ($WHSV_{fraction\ 3}$ = 1.6 $h^{-1}$, 1.8 h of time-on-stream).

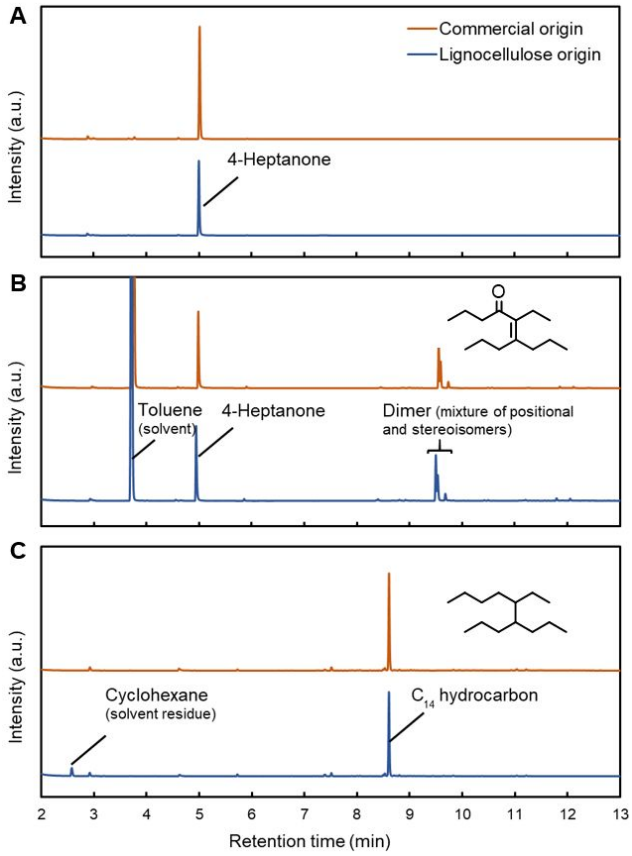


**Figure 5** GC-Polyarc/FID chromatograms of organic phase products from (A) ketonization, (B) condensation, and (C) HDO (solvent was removed from biologically derived product by distillation) when upgrading butyric acid through the integrated process scheme.

and dimer carbon yield to those using fresh ketone, confirming the initial feasibility of upgrading recycled ketone with solvent reuse (**Figure S10b)**. Fraction 3 from distillation comprised dimer (68% purity), heavier byproducts, and minor lighter components (e.g., 2 wt.% of 4-heptanone). The lower dimer purity compared to that in the single step conversion study (81% purity, **Figure 3**) illustrated the accumulation of non-target compounds from upstream conversion processes in the integrated conversion scheme. Fraction 3 was then used as the feed for the HDO reaction. Under the same operating conditions previously described with the exception of shorter time-on-stream, complete deoxygenation was achieved with selective conversion of dimer to the target $C_{14}$ hydrocarbon at 65% purity in the organic phase (**Figure 4**, **Scheme 3**). Organic phase non-target compounds included $C_{14}$ hydrocarbon isomers, other non-cyclic alkanes, cyclic alkanes, and a minor fraction of unsaturated structures (**Figures S11-S13**). The theoretical carbon yield for converting butyric acid to the target $C_{14}$ hydrocarbon is 88%. Assuming ideal separation during ketone recycling and complete mass recovery during sample transfer between reaction steps,[32] our experimental work demonstrates an overall carbon yield of 56% to the target $C_{14}$ hydrocarbon, which is 64% of the theoretical value. In comparison, the overall experimental carbon yield to the complex hydrocarbon mixture product was 86%, which is near theoretical due to minimal carbon losses to the gas phase. It is clear from these results that utilization of non-target hydrocarbons in the final diesel blendstock is critical to high carbon efficiency of the integrated process.

Finally, biologically-derived butyric acid was upgraded through the same integrated conversion scheme to demonstrate bioblendstock production from lignocellulosic biomass. Batch fermentation was performed with *Clostridium butyricum* on corn stover hydrolysate, the major components of which are glucose and xylose (**Table S5**).[69] Utilization of sugars in the hydrolysate was nearly complete after 56 h (**Figure S14a**), and butyric acid was produced at a final titer of 20.4 g $L^{-1}$ and yield of 0.32 g $g_{sugar}^{-1}$ (**Figure S14b**). A multi-step purification process recovered butyric acid from the fermentation broth at purity >99%, with separation efficiency and process cost to be further optimized.

Catalytic upgrading of the biologically-derived butyric acid achieved initial conversion efficiency and target product carbon yield comparable to those from upgrading commercial butyric acid (**Table 2**). For example, under the same ketonization and condensation conditions, conversion of the target reactants and carbon yield to the desired products deviated by <2% from model compound experiments. After condensation, solvent and unreacted ketone were removed through distillation as previously described. Due to limited volume of the biologically-derived substrate, the feed for HDO was diluted with cyclohexane to facilitate sample handling. Under the modified conditions, complete conversion of the dimer and production of an oxygen-free organic phase were still achieved, while the carbon yield to the target $C_{14}$ was lowered by 9%, potentially related to reduced WHSV. The concentrations of non-metallic and metallic impurities in the biologically-derived feed and organic phase products were consistently low (**Table S6**, variation of Si may be due to the wear of reactor coating), suggesting an insignificant impact on catalyst performance or product purity for the time scale studied. However, the variety and level of impurities can vary greatly depending on biological conversion and separation conditions,[70-72] and a systematic evaluation of their impact on downstream catalytic processes is needed to provide valuable information for further process integration with upstream processes. The target $C_{14}$ hydrocarbon was produced at 61% purity in the final hydrocarbon mixture product after solvent

(cyclohexane) removal, comparable with the results from upgrading commercial butyric acid. Carbon mass balance analysis was not performed due to limited volume of biologically-derived materials. However, both similar conversion performance (**Table 2**) and product gas chromatography profile (**Figure 5**) suggest that the carbon efficiency of upgrading biologically-derived butyric acid can be represented by those with commercial butyric acid, where the overall carbon yield to the final hydrocarbon mixture product was 86%.

### *Blendstock and Blend Fuel Properties Verification*

Fuel properties were first experimentally determined for a purified $C_{14}$ hydrocarbon blendstock to verify model predictions. The purified blendstock was obtained by removing non-target hydrocarbons using distillation to achieve a $C_{14}$ hydrocarbon purity of 94%. Measured boiling point, LHV, flash point, and YSI of the purified blendstock (**Table 3**) were well within 10% of the predicted values summarized in **Table 1**. Measured CN of an 81% $C_{14}$ blendstock also matched the model prediction very well. In contrast, the measured melting point was notably more than 40°C lower than the predicted value. A melting point or cloud point below -80°C indicates that this blendstock is likely suitable for use in even the coldest environments. Predicted values for melting point deviated substantially from experimental measurements. However, melting point prediction is inherently difficult, with mean prediction errors often exceeding 40°C.[73]

After verifying the purified $C_{14}$ hydrocarbon blendstock fuel properties, crude $C_{14}$ hydrocarbon blendstocks were evaluated following HDO conversion process without further purification. These crude products have lower $C_{14}$ hydrocarbon purity (e.g., 65% for crude product from upgrading commercial butyric acid) and are hereon referred to as "crude $C_{14}$ blendstock". The fuel properties were characterized to a similar extent to assess the impact of non-target compounds on neat blendstock and blended diesel fuel behavior. Compared with the purified blendstock, crude $C_{14}$ blendstock displayed similar bulk properties, such as LHV and density (**Table 3**), which was expected given the target $C_{14}$ hydrocarbon being the major component. In contrast to bulk properties, the crude $C_{14}$ blendstock exhibited a flash point 12°C lower than that of the purified $C_{14}$ blendstock (**Table 3**). As previously shown, hydrocarbons with lower boiling point tend to have lower flash point (**Figure S1c**). Therefore, the decrease in flash point was likely due to the short-chain hydrocarbons in the crude $C_{14}$ blendstock (<15 vol.% based on simulated distillation analysis), which resulted from HDO of 4-heptanone residue and undesired cracking reactions on acid catalysts. These low boiling point byproducts need to be monitored to ensure compliance with safety requirement. Nevertheless, the crude $C_{14}$ blendstock was well above the minimum flash point requirement for diesel fuels. To evaluate the sooting tendency of the crude $C_{14}$ blendstock on a volumetric basis that is consistent with volumetric blending, normalized soot concentration (NSC) was used. NSC is defined as the concentration of soot measured for a blendstock or a blend normalized to that of the base diesel (by definition having an NSC of 1). Both the purified and crude $C_{14}$ blendstocks exhibited NSC more than 50% lower than that of the base diesel, with the purified blendstock showing 21% lower NSC than the crude $C_{14}$ blendstock due to fewer non-target compounds (**Table 3**). Overall, these results validated the fuel properties of the crude $C_{14}$ blendstock and confirmed the successful conversion process development.

The promising fuel characteristics of the crude $C_{14}$ blendstock strongly indicate its suitability for use as drop-in diesel blendstock. This was further verified by measuring the fuel properties of a diesel blend containing a base diesel and 20 vol.% crude $C_{14}$ blendstock derived from bio-butyric acid. The base diesel is a petroleum diesel (commercial additives were removed) that has excellent properties including low cloud point and high energy density and cetane number (**Table 3 and S7**). When comparing the measured fuel properties between the blend and the base diesel, it was evident that the bioblendstock was able to maintain the base diesel quality (**Table 3**). For example, the bioblendstock slightly lowered the cloud point, demonstrating excellent solubility in the diesel fuel. The T90 was slightly reduced due to the lower boiling-range of the bioblendstock compared to the base diesel (**Figure S15**). Because the base diesel has a lower flash point than the blendstock, the flash point of the blend was dominated by that of the base diesel. The bioblendstock exhibited good ability to maintain diesel energy density compared with biodiesel and alcoholic diesel blendstocks,[74, 75] with only 5% reduction in blend LHV on either mass or volume basis. The measured CN of the blend was nearly unchanged and remained sufficiently beyond the minimum requirement of 40, which was expected considering the similar CN values between the base diesel and the blendstock.

It is notable that the bioblendstock demonstrated the potential to reduce diesel soot formation, with the blend reducing NSC by 11% compared with the base diesel (**Table 3**). In addition, NSC appeared to linearly decrease with the blending volume of $C_{14}$ blendstocks (**Figure S16**), suggesting the potential to further reduce diesel sooting by increasing the blend ratio.

**Table 3.** Measured fuel properties of $C_{14}$ blendstocks, base diesel, and a 20 vol.% blend.

| Properties | $C_{14}$ blendstock | | Diesel and blend | |
|---|---|---|---|---|
| | Purified | Crude[a] | Base diesel[b] | Blend[c] |
| Melting point (°C) | <-80 | ND | ND | ND |
| Cloud point (°C) | ND | <-80 | -9.7 | -12 |
| Boiling point (°C) | 230[d] | 266[e] | 333[e] | 327[e] |
| Flash point (°C) | 74 | 62[f] | 55 | 54[f] |
| LHV (MJ $kg^{-1}$) | 44 | 44 | 45 | 43 |
| LHV (MJ $L^{-1}$) | 34 | 34 | 39 | 37 |
| CN[g] | ND | 48[f] | 47 | 46[f] |
| YSI | 98 | NA | NA | NA |
| NSC | 0.37 | 0.47 | 1 | 0.89 |
| Viscosity (cSt) | ND | 1.49[f] | 2.66 | 2.08[f] |
| Density (g $mL^{-1}$) | 0.78 | 0.78 | 0.86 | 0.85 |

ND = Not determined. NA = Not applicable. [a]Derived from commercial butyric acid (65% $C_{14}$ purity). [b]Commercial additives were removed by clay treatment; see **Table S7** for additional fuel properties. [c]20 vol.% bio-butyric acid derived blendstock (61% $C_{14}$ purity) in base diesel. [d]Single boiling point. [e]T90 from simulated distillation profile. [f]20 vol.% 4-heptanone derived blendstock (81% $C_{14}$ purity). [g]Measured as indicated cetane number using ASTM method D8183.

## Discussion

To rationally target bioblendstocks that lead to advantageous properties, we leveraged fuel property prediction tools to inform the conversion pathway and molecule selection based on a "fuel property first" approach. This approach prioritizes fuel quality by estimating the fuel properties of potential products from an array of conversion pathways. We demonstrated this approach by employing a variety of empirical, predictive models derived from functional group contributions, molecular descriptors, and physical property correlations to screen 30 diesel-range hydrocarbon molecules accessible from short-chain $C_2$ and $C_4$ carboxylic acids derived from biological processes. This screening step allowed us to down-select butyric acid as the primary feedstock of interest for further catalytic upgrading to a non-cyclic branched $C_{14}$ hydrocarbon as a potentially high combustion efficiency, low soot formation diesel blendstock. Tailoring hydrocarbon diesel blendstock from biological-chemocatalytic conversion routes is only one example of the "fuel property first" approach. This approach can be applied to diverse conversion routes and molecules accessible from lignocellulosic biomass[76-80] to accelerate biofuel development, and the growing availability of fuel property prediction tools and metrics[12, 58, 81-83] can also guide design for a variety of fuel applications and combustion modes.

Fuel property predictive models enable low-cost rapid fuel property evaluation by removing the sample quantity constraints associated with experimental synthesis and testing. This allowed us to evaluate six fuel properties related to handling and storage, fuel economy, and combustion performance, all of which are critical to successful fuel deployment. Notably, the YSI predictive model made it possible to screen fuel molecules for their sooting tendency, which is an emerging fuel property metric to evaluate particulate emissions.[18-20] Comparing fuel property predictions across an array of molecule candidates narrowed the candidate pool from 30 down to 5 molecules; more importantly, it also provided quantitative information to facilitate further conversion pathway down-selection. Non-cyclic structures were identified as preferred targets for diesel applications, when compared to cyclic structures, due to the higher autoignition ability and lower sooting tendency of the former (**Figure S1e-f**). Fuel property measurements of the target $C_{14}$ hydrocarbon validated five out of six fuel property predictions, highlighting the value of the predictive models in rational fuel design.

Upgrading butyric acid through an integrated process scheme validated the conversion pathway and the advantageous fuel properties of the $C_{14}$ hydrocarbon. Meanwhile, conversion product analysis identified catalytic reaction byproducts as a key consideration for the "fuel property first" approach, which has rarely been addressed in fuel design. When producing the $C_{14}$ hydrocarbon from butyric acid through sequential reactions, multiple non-target hydrocarbons were accumulated in the crude conversion product (**Figures 4, S11-S13**) and entailed experimental evaluation of their influence on fuel properties. Although these non-target compounds did not significantly affect the bulk properties for the $C_{14}$ blendstock, minor components have the potential to dramatically impact fuel properties at low levels, such as depressing flash point by >10°C with <15 vol.% low boiling point byproducts (**Table 3**). These observations encourage future consideration of conversion byproducts in the early phase of fuel design, which may be achieved by estimating the properties of mixtures for selected fuel parameters. A critical consideration for designing blendstocks is their blending behavior, and linear mixing rules have often been assumed to simplify prediction methodology in fuel blend design studies.[13, 84, 85] This simple blending behavior has been experimentally observed for bulk properties such as CN and viscosity with hydrocarbon mixture,[86, 87] whereas non-ideal behaviors are frequently reported for other properties and oxygenate-hydrocarbon mixtures.[75, 88-90] For our bioblendstock blend, further testing is needed to determine the blend dependency since only single point blends measurements were performed. The ability to accurately predict mixture properties and blending relationships remains a grand challenge for computation and underscores the need to couple experimental validation of product fuel quality with the specific conversion routes and feedstocks of interest.

To further develop the butyric acid upgrading process we investigated, specific improvements can be made to each catalytic step. This work demonstrated complete butyric acid conversion with high molar selectivity (88%) to 4-heptanone under solvent-free and continuous process conditions with a commercial $ZrO_2$ catalyst. Similarly high yields have been shown in previous studies with acetic acid,[91, 92] and further improvement of selectivity may be possible by tuning operation conditions or metal oxide catalyst doping.[93, 94] Although deactivation was not observed at the time scale in this study, further work is needed to evaluate catalyst deactivation at longer time scales and varying biogenic carboxylic acid impurity profiles. Although we demonstrated promising single-pass batch reactor productivity with catalyst regeneration for 4-heptanone condensation over $Nb_2O_5$, it is important to note that significant reactivity differences exist between internal and terminal ketones. For example, the latter readily undergo aldol condensation over basic and amphoteric metal oxides, while internal ketones show little to no conversion.[30] The lower reactivity of internal ketones requires strongly acidic metal oxide catalysts with longer residence times and higher reaction temperatures, which can also lead to competing side reactions and fouling of strong acid active sites.[30, 95, 96] As such, it is important to better understand the mechanism and active site requirements for internal ketone condensation to improve yields and catalyst longevity. In addition, transitioning to flow reactor processing requires further development to reduce downtime, increase productivity, and improve process economics. Lastly, continuous HDO was demonstrated with very high initial selectivity (98%) to the target hydrocarbon, but reversible catalyst deactivation by fouling resulted in gradual decrease in selectivity. Further work is needed to identify if carbon deposition is caused by heavy compounds in the feed or in situ formation, as well as the impact on long term catalyst performance. Depending on the cause of deactivation, countermeasures can be taken such as pretreating the feed, tuning catalysts and process conditions, and controlling reaction rate regimes.[97, 98]

The three separate catalytic reaction steps demonstrated in this work provide a high degree of control over the conversion chemistry and final hydrocarbon blendstock fuel properties by optimization of each step. However, this approach has the drawback of requiring multiple reactors, distillation and recycle of unreacted ketones, and external solvent addition. In parallel, research is ongoing to intensify the catalytic upgrading process into a single reactor system with potential for reduced capital and operating costs.[31, 99-101] While promising, the consolidated approach currently has the limitation of lower hydrocarbon selectivity and less desirable final fuel properties for diesel applications. As such, further work is needed to assess the associated tradeoffs and necessary optimization required for co-developing conversion technology and advantaged diesel bioblendstocks. When considering overall process integration and techno-economics, work is ongoing to improve the biological and separation efficiency of short-chain carboxylic acids by identifying acid-tolerance organisms and integrating fermentation with *in situ* acid removal,[69, 72, 102, 103] as well as understand the impact of biogenic impurities on catalyst performance. A recent techno-economic analysis of an "n$^{th}$-plant" integrated biorefinery identified lignocellulosic sugars and their associated processing costs as major cost contributors for producing hydrocarbon fuels from the carboxylate platform.[103] As such, lignin valorization to co-products was necessary to achieve a minimum fuel selling price (MFSP) of <$3 per gallon of gasoline equivalent.[104-106] Fermentation, separation, and catalytic upgrading were found to contribute significantly less to the MFSP when compared to lignocellulosic sugars, offering potential to further reduce costs through the use of wet waste feedstocks (e.g., food waste, sludge, manure).[23, 24, 26, 107, 108]

Lastly, based on promising fuel property validation results, the $C_{14}$ blendstock warrants further engine testing to fully de-risk the bioblendstock from a fuel standpoint. Engine testing can assess fuel performance and quantify air pollutant emissions over a range of operating conditions reflective of use (e.g., compression ratio, air-fuel ratio, fuel injection pressure, cold starting).[109-111] Testing results can inform the "fuel property first" approach by improving our understanding of priority fuel property metrics that reflect desired engine and emission performance in actual use scenarios. Because traditional engine testing requires gallons of fuel, *in silico* and bench scale tools will be valuable to facilitating fuel performance evaluation. Bench scale evaluation of combustion kinetics can be performed with samples on the order of several hundred milliliters of bioblendstock,[112, 113] and these data can serve as the basis for kinetic simulations that could ultimately be used – in reduced form – as part of an engine simulation to predict efficiency and approximate emissions effects.[114, 115] Bench scale studies of fuel sprays and measurement of related properties can also inform these simulations.[116] Together with fuel property predictive models, these strategies can further accelerate the development of performance-advantaged bioblendstocks for diesel engines.

# Conclusions

Advancement of renewable biofuels requires high quality bioblendstocks accessible from low-cost feedstocks with efficient conversion pathways. Here, we demonstrated a "fuel property first" design approach to access low-sooting, drop-in hydrocarbon diesel bioblendstock from lignocellulose derived short-chain carboxylic acids. By leveraging predictive models, critical fuel properties were rapidly screened for an array of hydrocarbons accessible from $C_2/C_4$ acids, leading to a down-selected conversion pathway targeting a non-cyclic branched $C_{14}$ hydrocarbon molecule, 5-ethyl-4-propylnonane. Catalytic upgrading of butyric acid through an integrated process scheme showed high selectivity (>80%) for individual conversion steps, and >80% of the carbon in the acid feed was captured by a hydrocarbon mixture product with >60% purity of the target $C_{14}$ hydrocarbon (56% overall carbon yield to the target $C_{14}$ hydrocarbon). The majority of fuel property predictions were verified using a purified $C_{14}$ blendstock, and the crude conversion product exhibited similar bulk properties, validating the impact of fuel property predictive models on developing high-quality, low-sooting tendency diesel bioblendstocks. Furthermore, blending of the $C_{14}$ bioblendstock into a base diesel at 20 vol.% confirmed its suitability for use as a drop-in diesel blendstock, leading to >10% reduction in sooting tendency of the blend. Overall, this work demonstrates the potential of a "fuel property first" design approach to inform conversion pathway development towards cleaner-burning renewable fuels with lower environmental and human health impacts.

# Materials and methods

### *Predictive models*

Two models were used to estimate melting point. The first was sourced from commercial software, ChemDraw Professional 15.1 (PerkinElmer) which exploits both Joback's fragmentation method as well as Stein's modification to Joback's method.[40] The second prediction was obtained from the estimation program MPBPWIN™ in EPI Suite™ (US EPA, Syracuse Research Corp.).[41] This program estimates melting point by giving a weighted average of the results of two methods, the Joback Method (a group contribution method) and the Gold and Ogle method (a correlation between melting point and boiling point). Boiling point predictions also utilized the ChemDraw and EPI Suite tools, with the addition of a third available predictive model developed by Satou et al.[43] Flashpoint was estimated via two predictive models, both requiring a reliable boiling point. One of the earliest was developed by Butler et al.,[44] which was built on correlation for petroleum boiling in the range of about 90 to 370°C. The second correlation was later developed by Prugh and based on a larger database of hydrocarbons and fuel mixtures.[45] Numerous predictive models for the higher heating value for a variety of samples have been developed, primarily based around species mass contributions. The first model applied in this work is the Dulong equation, which was used to determine higher heating value estimates for coal and fossil fuels.[49] This work also includes two predictive estimates which are from modifications to Dulong's formula. Lloyd and Davenport[50] included ethers and other oxygenates in their modification, and Boie[51] adapted the formula for a larger

dataset. Lower heating values reported here are determined by the following equation, which is a function of the estimated mass% hydrogen (H) in a sample (ASTM D240, Section 10.5.1).[117]

$$LHV = HHV - (0.2122*H) \quad (1)$$

Cetane number predictions were produced using a back-propagating artificial neural network (ANN) with inputs including experimental CN values and quantitative structure-property relationships (QSPR) for individual molecules. The model uses an iterative regression analysis technique to reduce the number of input parameters; in the case of CN, from >1500 to 15. The ANN randomly assigns an individual molecule from the known data set to one of three conditions: learning, validation, and testing, with proportions of 65%, 25%, and 10% respectively. The trained model is subsequently applied to the new molecule of interest's QSPR parameters in order to produce a predicted CN. The method has been shown to provide high accuracy and repeatability across a broad range of hydrocarbons when predicting CN.[52, 53] Yield sooting index predictions were generated using a group contribution model that sums contributions from each carbon atom.[19]

### *Catalytic upgrading*

Commercial butyric acid, 4-heptanone, toluene and cyclohexane were purchased from standard chemical suppliers such as Sigma-Aldrich or Acros. Biologically derived butyric acid was obtained from lignocellulosic sugars fermentation as detailed in the Supporting Information.

Fresh catalysts and selected post-reaction catalysts were characterized by $N_2$ physisorption, ammonia TPD, pyridine DRIFTS, chemisorption, and TGA-IR. Details on catalyst synthesis and characterization methods are provided in the Supporting Information.

Packed-bed reactor experiments were performed in a stainless-steel tubular reactor system. The reactor tube was coated with a silica Dursan coating provided by SilcoTek Coating Co. Batch reactor experiments were performed in a Parr multi-batch reactor system (Parr Instrument Co.), and the reactors were also coated with the silica Dursan coating. Liquid products were analyzed by gas chromatography with a flame ionization detector and a mass spectrometer (GC-FID/MS). Carbon, hydrocarbon, nitrogen, sulfur, and metals analyses were performed by Huffman Hazen Laboratories. Selected samples were analyzed by high resolution mass spectrometry, nuclear magnetic resonance spectroscopy, and two-dimensional gas chromatography with time-of-flight mass spectrometry (GC×GC-TOFMS). Further details on catalytic testing systems, data analysis, and analytical methods were provided in the Supporting Information.

### *Fuel property testing*

Cetane number was measured as indicated cetane number using 40 mL of sample in an AFIDA instrument (ASTM D8183). Boiling point was estimated using simulated distillation (D2887). A single boiling point value was reported for the purified $C_{14}$ blendstock due to its relatively high purity (94%), and T90 (distillation temperature at 90% recovered) was reported for mixtures, including the crude $C_{14}$ blendstock, base diesel, and blend. Higher heating value was measured by combusting samples in a bomb calorimeter (D240), with hydrogen content used to calculate lower heating value being measured for each sample using a LECO TruSpec CHN determinator. Samples were combusted at 950°C under a flow of excess oxygen and the gas produced was analyzed with infrared spectroscopy to quantify the amount of $CO_2$ and $H_2O$ produced. Ethylenediaminetetraacetic acid (EDTA) was used as the calibration standard. Density was found using a Mettler-Toledo DM40 density meter (D4052). Viscosity was measured at 40°C using D445 or a TA Instrument AR1500 equipped with a recessed rotor at a shear rate of 1-100 $s^{-1}$. Melting point (for pure compouds) and cloud point (for mixtures) were measured using a Phase Technology Series 70X (a modified version of D5773). Flash point was measured using D7094. Two different types of sooting tendency measurements were performed. Measurement of YSI followed published procedures.[118] Briefly, samples of the test substance, n-heptane, and toluene were doped into the fuel of a methane/air nonpremixed flame at a mole fraction of 1000 ppm. Soot concentrations in the resulting flames were quantified with line-of-sight spectral radiance (LSSR). The maximum LSSR in each flame was then converted to a YSI by a linear rescaling with the specified endpoints of n-heptane = 36.0 YSI units and toluene = 170.9 YSI units. To obtain normalized soot concentration (NSC), the same procedures were followed except that all of the dopants were added at a fixed volumetric flowrate of 100 μL $h^{-1}$. The results were not indexed to toluene and heptane; instead the soot concentration from the undoped flame was subtracted off and then the concentration attributable to the dopant was normalized to the value for the reference base diesel fuel.

## Conflicts of interest

There are no conflicts to declare.

## Acknowledgements

We would like to thank Darren J. Peterson for conducting sugars and acids analyses from the bioreactor cultivations. We highly appreciate the help from Davis R. Conklin and Stephen M. Tifft with batch testing and distillation. A portion of this research was conducted as part of the Co-Optimization of Fuels & Engines (Co-Optima) project sponsored by the U.S. Department of Energy – Office of Energy Efficiency and Renewable Energy, Bioenergy Technologies and Vehicle Technologies Offices. Co-Optima is a collaborative project of several national laboratories initiated to simultaneously accelerate the introduction of affordable, scalable, and sustainable biofuels and high-efficiency, low-emission vehicle engines. Work at the National Renewable Energy Laboratory was performed under Contract No. DE347AC36-99GO10337. Part of this work was also supported by Co-Optima through Program Award Number DE-EE0007983. P.A.C.'s participation was supported by an NSF Research Experiences for Undergraduates supplement to Grant Number CBET 1604983. A portion of this research was also conducted as part of the Chemical Catalysis for Bioenergy Consortium through Contract No. DE-AC36-08GO28308 at the National Renewable Energy Laboratory. The views expressed in the article do not necessarily represent the views of the U.S.

Department of Energy or the U.S. Government. The U.S. Government retains and the publisher, by accepting the article for publication, acknowledges that the U.S. Government retains a nonexclusive, paid-up, irrevocable, worldwide license to publish or reproduce the published form of this work, or allow others to do so, for U.S. Government purposes.

## References


1. *World Energy Look*, International Energy Agency, London, UK, 2017.
2. *Tracking Clean Energy Progress*, International Energy Agency, 2017.
3. *The Future of Trucks Implications for Energy and the Environment*, International Energy Agency, 2017.
4. M. H. Langholtz, B. J. Stokes and L. M. Eaton, *2016 Billion-Ton Report: Advancing Domestic Resources for a Thriving Bioeconomy, Volume 1: Economic Availability of Feedstocks*, U.S. Department of Energy Oak Ridge National Laboratory, 2016.
5. J. C. Serrano-Ruiz and J. A. Dumesic, *Energy & Environmental Science*, 2011, **4**, 83-99.
6. S. Shylesh, A. A. Gokhale, C. R. Ho and A. T. Bell, *Accounts of Chemical Research*, 2017, **50**, 2589-2597.
7. Y. Shen, L. Jarboe, R. Brown and Z. Wen, *Biotechnology Advances*, 2015, **33**, 1799-1813.
8. R. Gani, C. Jiménez-González and D. J. C. Constable, *Computers & Chemical Engineering*, 2005, **29**, 1661-1676.
9. L. Y. Ng, F. K. Chong and N. G. Chemmangattuvalappil, *Computers & Chemical Engineering*, 2015, **81**, 115-129.
10. S. J. Y. Macalino, V. Gosu, S. Hong and S. Choi, *Archives of Pharmacal Research*, 2015, **38**, 1686-1701.
11. N. D. Austin, N. V. Sahinidis and D. W. Trahan, *Chemical Engineering Research and Design*, 2016, **116**, 2-26.
12. M. Dahmen and W. Marquardt, *Energy & Fuels*, 2016, **30**, 1109-1134.
13. M. Dahmen and W. Marquardt, *Energy & Fuels*, 2017, **31**, 4096-4121.
14. W. L. Kubic, R. W. Jenkins, C. M. Moore, T. A. Semelsberger and A. D. Sutton, *Industrial & Engineering Chemistry Research*, 2017, **56**, 12236-12245.
15. J. Hansen and L. Nazarenko, *Proceedings of the National Academy of Sciences of the United States of America*, 2004, **101**, 423-428.
16. A. Wierzbicka, P. T. Nilsson, J. Rissler, G. Sallsten, Y. Xu, J. H. Pagels, M. Albin, K. Österberg, B. Strandberg, A. Eriksson, M. Bohgard, K. Bergemalm-Rynell and A. Gudmundsson, *Atmospheric Environment*, 2014, **86**, 212-219.
17. C. S. McEnally and L. D. Pfefferle, *Combustion and Flame*, 2007, **148**, 210-222.
18. D. D. Das, C. S. McEnally, T. A. Kwan, J. B. Zimmerman, W. J. Cannella, C. J. Mueller and L. D. Pfefferle, *Fuel*, 2017, **197**, 445-458.
19. D. D. Das, P. C. St. John, C. S. McEnally, S. Kim and L. D. Pfefferle, *Combustion and Flame*, 2018, **190**, 349-364.
20. P. C. St. John, P. Kairys, D. D. Das, C. S. McEnally, L. D. Pfefferle, D. J. Robichaud, M. R. Nimlos, B. T. Zigler, R. L. McCormick, T. D. Foust, Y. J. Bomble and S. Kim, *Energy & Fuels*, 2017, **31**, 9983-9990.
21. A. J. J. Straathof, *Chemical Reviews*, 2014, **114**, 1871-1908.
22. M. Sjöblom, L. Matsakas, P. Christakopoulos and U. Rova, *FEMS Microbiology Letters*, 2016, **363**, fnw064.
23. M. A. Khan, H. H. Ngo, W. S. Guo, Y. Liu, L. D. Nghiem, F. I. Hai, L. J. Deng, J. Wang and Y. Wu, *Bioresource Technology*, 2016, **219**, 738-748.
24. M. T. Agler, B. A. Wrenn, S. H. Zinder and L. T. Angenent, *Trends in Biotechnology*, 2011, **29**, 70-78.
25. I. Vassilev, P. A. Hernandez, P. Batlle-Vilanova, S. Freguia, J. O. Krömer, J. Keller, P. Ledezma and B. Virdis, *ACS Sustainable Chemistry & Engineering*, 2018, **6**, 8485-8493.
26. R. Moscoviz, E. Trably, N. Bernet and H. Carrère, *Green Chemistry*, 2018, **20**, 3159-3179.
27. E. R. Sacia, M. Balakrishnan, M. H. Deaner, K. A. Goulas, F. D. Toste and A. T. Bell, *ChemSusChem*, 2015, **8**, 1726-1736.
28. M. J. Climent, A. Corma and S. Iborra, *Green Chemistry*, 2014, **16**, 516-547.
29. D. M. Alonso, J. Q. Bond and J. A. Dumesic, *Green Chemistry*, 2010, **12**, 1493-1513.
30. S. Shylesh, A. A. Gokhale, K. Sun, A. Grippo, D. Jadhav, A. Yeh, C. R. Ho and A. T. Bell, *Sustainable Energy & Fuels*, 2017, **1**, 1805-1809.
31. B. Rozmysłowicz, J. H. Yeap, A. M. I. Elkhaiary, M. Talebi Amiri, R. L. Shahab, Y. M. Questell-Santiago, C. Xiros, B. P. Le Monnier, M. H. Studer and J. S. Luterbacher, *Green Chemistry*, 2019, **21**, 2801-2809.
32. H. Olcay, A. V. Subrahmanyam, R. Xing, J. Lajoie, J. A. Dumesic and G. W. Huber, *Energy & Environmental Science*, 2013, **6**, 205-216.
33. A. Deneyer, E. Peeters, T. Renders, S. Van den Bosch, N. Van Oeckel, T. Ennaert, T. Szarvas, T. I. Korányi, M. Dusselier and B. F. Sels, *Nature Energy*, 2018, **3**, 969–977.
34. Y.-S. Jang, J. A. Im, S. Y. Choi, J. I. Lee and S. Y. Lee, *Metabolic Engineering*, 2014, **23**, 165-174.
35. O. Nagashima, S. Sato, R. Takahashi and T. Sodesawa, *Journal of Molecular Catalysis A: Chemical*, 2005, **227**, 231-239.
36. C. A. Gaertner, J. C. Serrano-Ruiz, D. J. Braden and J. A. Dumesic, *Journal of Catalysis*, 2009, **266**, 71-78.
37. M. Balakrishnan, E. R. Sacia, S. Sreekumar, G. Gunbas, A. A. Gokhale, C. D. Scown, F. D. Toste and A. T. Bell, *Proceedings of the National Academy of Sciences*, 2015, **112**, 7645-7649.

38. R. W. Jenkins, C. M. Moore, T. A. Semelsberger, C. J. Chuck, J. C. Gordon and A. D. Sutton, *ChemSusChem*, 2016, **9**, 922-931.
39. D. J. Gaspar, R. L. McCormick, E. Polikarpov, G. Fioroni, A. George and K. O. Albrecht, *Functional Group Analysis for Diesel-like Mixing-Controlled Compression Ignition Combustion Blendstocks*, Pacific Northwest National Lab.(PNNL), Richland, WA (United States), 2016.
40. http://www.cambridgesoft.com/support/DesktopSupport/Documentation/Manuals/files/chemdraw_9_english.pdf.
41. *Estimation Programs Interface Suite™ for Microsoft® Windows, v 4.11*, United States Environmental Protection Agency, Washington, DC, USA, 2018.
42. *ASTM International, "Standard Specification for Diesel Fuel Oils"*, 2018.
43. M. Satou, S. Yokoyama and Y. Sanada, *Fuel*, 1992, **71**, 565-574.
44. R. M. Butler, G. M. Cooke, G. G. Lukk and B. G. Jameson, *Industrial & Engineering Chemistry*, 1956, **48**, 808-812.
45. R. W. Prugh, *Journal of Chemical Education*, 1973, **50**, A85.
46. S. K. Hoekman, A. Broch, C. Robbins, E. Ceniceros and M. Natarajan, *Renewable and Sustainable Energy Reviews*, 2012, **16**, 143-169.
47. *Diesel Fuels Technical Review*, Chevron Global Marketing, 2007.
48. D. A. Saldana, L. Starck, P. Mougin, B. Rousseau, L. Pidol, N. Jeuland and B. Creton, *Energy & Fuels*, 2011, **25**, 3900-3908.
49. R. Mott and C. Spooner, *Fuel*, 1940, **19**, 242.
50. W. G. Lloyd and D. A. Davenport, *Journal of Chemical Education*, 1980, **57**, 56.
51. W. Boie, *Energietechnik*, 1953, **3**, 309-316.
52. T. Kessler and J. H. Mack, *The Journal of Open Source Software*, 2017, **2**, 401.
53. T. Kessler, E. R. Sacia, A. T. Bell and J. H. Mack, *Fuel*, 2017, **206**, 171-179.
54. *DIN EN 590 Automotive fuels - Diesel - Requirements and test methods (includes Amendment: 2017)*, Deutsches Institut fur Normung E.V. (DIN), 2017.
55. C. T. O'Connor, R. D. Forrester and M. S. Scurrell, *Fuel*, 1992, **71**, 1323-1327.
56. S. M. Heck, H. O. Pritchard and J. F. Griffiths, *Journal of the Chemical Society, Faraday Transactions*, 1998, **94**, 1725-1727.
57. C. K. Westbrook, *Proceedings of the Combustion Institute*, 2000, **28**, 1563-1577.
58. M. Dahmen and W. Marquardt, *Energy & Fuels*, 2015, **29**, 5781-5801.
59. C. S. McEnally and L. D. Pfefferle, *Environmental Science & Technology*, 2011, **45**, 2498-2503.
60. K. O. Johansson, M. P. Head-Gordon, P. E. Schrader, K. R. Wilson and H. A. Michelsen, *Science*, 2018, **361**, 997-1000.
61. T. N. Pham, T. Sooknoi, S. P. Crossley and D. E. Resasco, *ACS Catalysis*, 2013, **3**, 2456-2473.
62. E. L. Kunkes, E. I. Gürbüz and J. A. Dumesic, *Journal of Catalysis*, 2009, **266**, 236-249.
63. S. Shylesh, D. Kim, A. A. Gokhale, C. G. Canlas, J. O. Struppe, C. R. Ho, D. Jadhav, A. Yeh and A. T. Bell, *Industrial & Engineering Chemistry Research*, 2016, **55**, 10635-10644.
64. G. S. Foo, D. Wei, D. S. Sholl and C. Sievers, *ACS Catalysis*, 2014, **4**, 3180-3192.
65. C. R. Ho, S. Zheng, S. Shylesh and A. T. Bell, *Journal of Catalysis*, 2018, **365**, 174-183.
66. B. Ashish, S. Basudeb and A.-O. M. M., *ChemSusChem*, 2015, **8**, 4022-4029.
67. H. Li, A. Riisager, S. Saravanamurugan, A. Pandey, R. S. Sangwan, S. Yang and R. Luque, *ACS Catalysis*, 2018, **8**, 148-187.
68. T. Okuhara, *Chemical Reviews*, 2002, **102**, 3641-3666.
69. R. Nelson, D. Peterson, E. Karp, G. Beckham and D. Salvachúa, *Fermentation*, 2017, **3**, 10.
70. S. V. Vassilev, D. Baxter, L. K. Andersen, C. G. Vassileva and T. J. Morgan, *Fuel*, 2012, **94**, 1-33.
71. D. R. Vardon, N. A. Rorrer, D. Salvachua, A. E. Settle, C. W. Johnson, M. J. Menart, N. S. Cleveland, P. N. Ciesielski, K. X. Steirer, J. R. Dorgan and G. T. Beckham, *Green Chemistry*, 2016, **18**, 3397-3413.
72. E. M. Karp, R. M. Cywar, L. P. Manker, P. O. Saboe, C. T. Nimlos, D. Salvachúa, X. Wang, B. A. Black, M. L. Reed, W. E. Michener, N. A. Rorrer and G. T. Beckham, *ACS Sustainable Chemistry & Engineering*, 2018, **6**, 15273-15283.
73. L. D. Hughes, D. S. Palmer, F. Nigsch and J. B. O. Mitchell, *Journal of Chemical Information and Modeling*, 2008, **48**, 220-232.
74. A. Murugesan, C. Umarani, R. Subramanian and N. Nedunchezhian, *Renewable and Sustainable Energy Reviews*, 2009, **13**, 653-662.
75. M. Lapuerta, R. García-Contreras, J. Campos-Fernández and M. P. Dorado, *Energy & Fuels*, 2010, **24**, 4497-4502.
76. J. G. Linger, D. R. Vardon, M. T. Guarnieri, E. M. Karp, G. B. Hunsinger, M. A. Franden, C. W. Johnson, G. Chupka, T. J. Strathmann, P. T. Pienkos and G. T. Beckham, *Proceedings of the National Academy of Sciences*, 2014, **111**, 12013-12018.
77. T. J. Schwartz, B. J. O'Neill, B. H. Shanks and J. A. Dumesic, *ACS Catalysis*, 2014, **4**, 2060-2069.
78. R. Xing, A. V. Subrahmanyam, H. Olcay, W. Qi, G. P. van Walsum, H. Pendse and G. W. Huber, *Green Chemistry*, 2010, **12**, 1933-1946.
79. A. Deneyer, T. Renders, J. Van Aelst, S. Van den Bosch, D. Gabriëls and B. F. Sels, *Current Opinion in Chemical Biology*, 2015, **29**, 40-48.
80. B. Op de Beeck, M. Dusselier, J. Geboers, J. Holsbeek, E. Morré, S. Oswald, L. Giebeler and B. F.

Sels, *Energy & Environmental Science*, 2015, **8**, 230-240.
81. L. S. Whitmore, R. W. Davis, R. L. McCormick, J. M. Gladden, B. A. Simmons, A. George and C. M. Hudson, *Energy & Fuels*, 2016, **30**, 8410-8418.
82. R. McCormick, G. Fioroni, L. Fouts, E. Christensen, J. Yanowitz, E. Polikarpov, K. Albrecht, D. Gaspar, J. Gladden and A. George, *SAE Int. J. Fuels Lubr.*, 2017, **10**, 442-460.
83. G. Fioroni, L. Fouts, J. Luecke, D. Vardon, N. Huq, E. Christensen, X. Huo, T. Alleman, R. McCormick, M. Kass, E. Polikarpov, G. Kukkadapu and R. A. Whitesides, SAE Technical Paper 2019-01-0570, 2019.
84. N. A. Yunus, K. V. Gernaey, J. M. Woodley and R. Gani, *Computers & Chemical Engineering*, 2014, **66**, 201-213.
85. S. Kalakul, L. Zhang, Z. Fang, H. A. Choudhury, S. Intikhab, N. Elbashir, M. R. Eden and R. Gani, *Computers & Chemical Engineering*, 2018.
86. P. Ghosh and S. B. Jaffe, *Industrial & Engineering Chemistry Research*, 2006, **45**, 346-351.
87. M. Lapuerta, M. Villajos, J. R. Agudelo and A. L. Boehman, *Fuel Processing Technology*, 2011, **92**, 2406-2411.
88. L. Canoira, J. García Galeán, R. Alcántara, M. Lapuerta and R. García-Contreras, *Renewable Energy*, 2010, **35**, 208-217.
89. M. L. Botero, Y. Huang, D. L. Zhu, A. Molina and C. K. Law, *Fuel*, 2012, **94**, 342-347.
90. L. Y. Phoon, A. A. Mustaffa, H. Hashim and R. Mat, *Industrial & Engineering Chemistry Research*, 2014, **53**, 12553-12565.
91. R. Martinez, M. C. Huff and M. A. Barteau, *Journal of Catalysis*, 2004, **222**, 404-409.
92. M. Gliński, J. Kijeński and A. Jakubowski, *Applied Catalysis A: General*, 1995, **128**, 209-217.
93. K. M. Dooley, A. K. Bhat, C. P. Plaisance and A. D. Roy, *Applied Catalysis A: General*, 2007, **320**, 122-133.
94. T. N. Pham, D. Shi and D. E. Resasco, *Journal of Catalysis*, 2014, **314**, 149-158.
95. J. E. Rekoske and M. A. Barteau, *Industrial & Engineering Chemistry Research*, 2011, **50**, 41-51.
96. O. Kikhtyanin, V. Kelbichová, D. Vitvarová, M. Kubů and D. Kubička, *Catalysis Today*, 2014, **227**, 154-162.
97. M. Argyle and C. Bartholomew, *Catalysts*, 2015, **5**, 145.
98. J.-P. Lange, *Angewandte Chemie International Edition*, 2015, **54**, 13186-13197.
99. E. L. Kunkes, D. A. Simonetti, R. M. West, J. C. Serrano-Ruiz, C. A. Gärtner and J. A. Dumesic, *Science*, 2008, **322**, 417-421.
100. E. I. Gürbüz, E. L. Kunkes and J. A. Dumesic, *Applied Catalysis B: Environmental*, 2010, **94**, 134-141.
101. E. I. Gürbüz, E. L. Kunkes and J. A. Dumesic, *Green Chemistry*, 2010, **12**, 223-227.
102. P. O. Saboe, L. P. Manker, W. E. Michener, D. J. Peterson, D. G. Brandner, S. P. Deutch, M. Kumar, R. M. Cywar, G. T. Beckham and E. M. Karp, *Green Chemistry*, 2018, **20**, 1791-1804.
103. R. E. Davis, N. J. Grundl, L. Tao, M. J. Biddy, E. C. Tan, G. T. Beckham, D. Humbird, D. Thompson and M. S. Roni, *Design and Economics for the Conversion of Lignocellulosic Biomass to Hydrocarbon Fuels and Coproducts: 2018 Biochemical Design Case Update; Biochemical Deconstruction and Conversion of Biomass to Fuels and Products via Integrated Biorefinery Path*, National Renewable Energy Lab. (NREL), Golden, CO, USA, 2018.
104. G. T. Beckham, C. W. Johnson, E. M. Karp, D. Salvachúa and D. R. Vardon, *Current Opinion in Biotechnology*, 2016, **42**, 40-53.
105. A. Corona, M. J. Biddy, D. R. Vardon, M. Birkved, M. Z. Hauschild and G. T. Beckham, *Green Chemistry*, 2018, **20**, 3857-3866.
106. A. E. Settle, L. Berstis, S. Zhang, N. A. Rorrer, H. Hu, R. M. Richards, G. T. Beckham, M. F. Crowley and D. R. Vardon, *ChemSusChem*, 2018, **0**.
107. R. L. Skaggs, A. M. Coleman, T. E. Seiple and A. R. Milbrandt, *Renewable and Sustainable Energy Reviews*, 2018, **82**, 2640-2651.
108. A. Badgett, E. Newes and A. Milbrandt, *Energy*, 2019, **176**, 224-234.
109. M. Happonen, J. Heikkilä, T. Murtonen, K. Lehto, T. Sarjovaara, M. Larmi, J. Keskinen and A. Virtanen, *Environmental Science & Technology*, 2012, **46**, 6198-6204.
110. A. Prokopowicz, M. Zaciera, A. Sobczak, P. Bielaczyc and J. Woodburn, *Environmental Science & Technology*, 2015, **49**, 7473-7482.
111. A. M. Ashraful, H. H. Masjuki, M. A. Kalam, I. M. Rizwanul Fattah, S. Imtenan, S. A. Shahir and H. M. Mobarak, *Energy Conversion and Management*, 2014, **80**, 202-228.
112. C. L. Barraza-Botet, J. Luecke, B. T. Zigler and M. S. Wooldridge, *Fuel*, 2018, **224**, 401-411.
113. S. S. Goldsborough, J. Santner, D. Kang, A. Fridlyand, T. Rockstroh and M. C. Jespersen, *Proceedings of the Combustion Institute*, 2018.
114. G. Kukkadapu, D. Kang, S. W. Wagnon, K. Zhang, M. Mehl, M. Monge-Palacios, H. Wang, S. S. Goldsborough, C. K. Westbrook and W. J. Pitz, *Proceedings of the Combustion Institute*, 2018.
115. C. K. Westbrook, M. Mehl, W. J. Pitz, G. Kukkadapu, S. Wagnon and K. Zhang, *Physical Chemistry Chemical Physics*, 2018, **20**, 10588-10606.
116. S. Daly, E. Cenker, L. Pickett and S. Skeen, *SAE International*, 2018.
117. *ASTM D240-17, Standard Test Method for Heat of Combustion of Liquid Hydrocarbon Fuels by Bomb Calorimeter*, ASTM International, West Conshohocken, PA, 2017.
118. C. S. McEnally, Y. Xuan, P. C. St. John, D. D. Das, A. Jain, S. Kim, T. A. Kwan, L. K. Tan, J. Zhu and L.

D. Pfefferle, *Proceedings of the Combustion Institute*, 2018.